

LOW BETA ELLIPTICAL CAVITIES FOR PULSED AND CW OPERATION*

Paolo Pierini, Serena Barbanotti, Angelo Bosotti, Paolo Michelato, Laura Monaco, Rocco Paparella
INFN Milano LASA, Segrate MI, Italy

Abstract

The two TRASCO elliptical superconducting cavities for low energy (100-200 MeV) protons have been completed by equipping them with cold tuner and a magnetic shield internal to the Helium tank. One of the two structures is now available for significant tests of Lorentz Force Detuning control of these low beta structures under pulsed conditions for future high intensity linac programs, as SPL or the ESS. The second structure will be integrated in a single cavity cryomodule under fabrication for the prototypical activities of the EUROTRANS program for nuclear waste transmutation in accelerator driven systems.

CAVITY PREPARATION FOR HORIZONTAL TESTING

The two TRASCO five-cell elliptical superconducting cavities [1] have been equipped with the ancillary components needed for qualification in a horizontal cryostat. A Ti Helium tank has been welded to the cavity, with the necessary magnetic shielding inserted in its inner space [2], and a cold tuning system of the blade-type has been fabricated [3]. Both cavities outreached their nominal specifications (8.5 MV/m of accelerating field at a Q value $> 5 \cdot 10^9$) with a considerable operational margin in vertical tests [4] and the completion of the dressed cavity package will allow performing the qualification of the multicell structures in testing conditions similar to the operation in a linac environment.

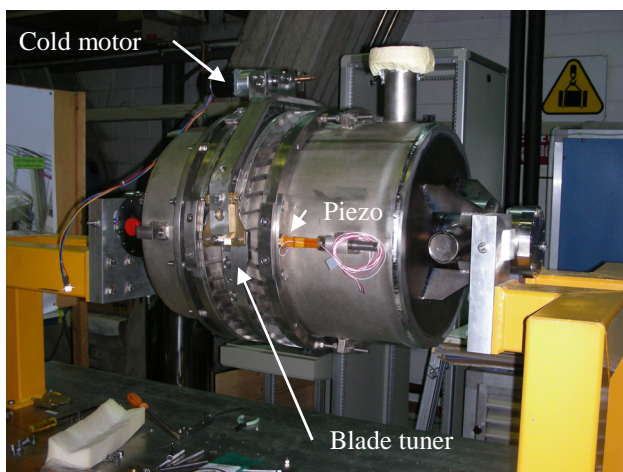


Figure 1: The TRASCO cavity equipped with Helium tank and blade tuner in the warm test stand.

* This work has been partially supported by the EURATOM EC FP6 under contract FI6KW-CT-2004-516520 (EUROTRANS), by the EC FP6 program CARE (contract number RII3-CT-2003-506395) and by the FP7 program SLHC-PP (contract number 212114)

The coaxial blade tuner designed for the TRASCO cavities (and derived from the type proposed for the ILC [5]) allows both a slow and a fast piezo-assisted tuning action for dynamic compensation of the Lorentz force detuning in pulsed operation or microphonic stabilization in CW operation.

One cavity will be tested for high power pulsed operation for Lorentz Force Detuning compensation experiments in CRYHOLAB at Saclay for the SLHC-PP FP7 program while the second will be tested in high power CW operation, with microphonics control, in a prototypical cryomodule for ADS activities at Orsay, for the EUROTRANS FP6 program.

THE INNER MAGNETIC SHIELD

In both conditions foreseen for the cavities, the earth magnetic field needs to be shielded efficiently from the niobium cavity surfaces in order not to increase the surface resistivity due to field trapping, limiting the cavity performances. The coaxial tuner is located outside the cavity He tank, thus to minimize the dimension and costs of the magnetic shield enclosure. Therefore we choose to design a magnetic shield located internally to the cavity He tank. This solution leads to simple and effective shield design and cavity package assembly procedures.

Required Shielding Factor

The wall losses on the cavity surfaces are determined by the niobium surface resistance, which has contributions arising from several physical phenomena:

$$R_{surf} = R_{BCS}(v, T) + R_{res} + R_{mag}(H_{ext}) \quad (1)$$

The first fundamental term (R_{BCS}) comes from the BCS theory and depends on the temperature and to the square on the RF frequency [6]. At 704.4 MHz and 2 K operation the BCS term accounts for 3.2 nΩ.

The second term, the residual resistance, is related to the technology of the cavity fabrication and treatment processes and can arise from various sources (foreign material inclusions during fabrication, residues of chemical etching, condensed gases, ...).

The comparison of the overall surface resistance measurements derived from the vertical RF tests with the fit to the BCS model gave us an estimation of the residual resistance term in the range of a few (5-7) nΩ [4].

Finally, the last term is due to the pinning and trapping of DC magnetic flux (the earth magnetic field) in the material. For high RRR niobium :

$$R_{mag} = 3[\text{n}\Omega] \langle H_{ext} [\mu\text{T}] \rangle \sqrt{v [\text{GHz}]} \quad (2)$$

where $\langle H_{ext} \rangle$ is the average magnetic field flux seen by the cavity surface and v the cavity RF frequency.

Finally, the surface resistance and the quality factor of the resonator are related through the cavity geometrical factor $G=R_{surf} Q$, which for the TRASCO cavity has the value of 160Ω . Figure 3 shows the expected Q as a function of the magnetic surface contribution to the total resistivity (for the two values of the residual resistance determined from the RF tests). The nominal Q value of $5 \cdot 10^9$ is reached at $20 \text{ n}\Omega$, i.e. at approximately $8 \mu\text{T}$ average surface field.

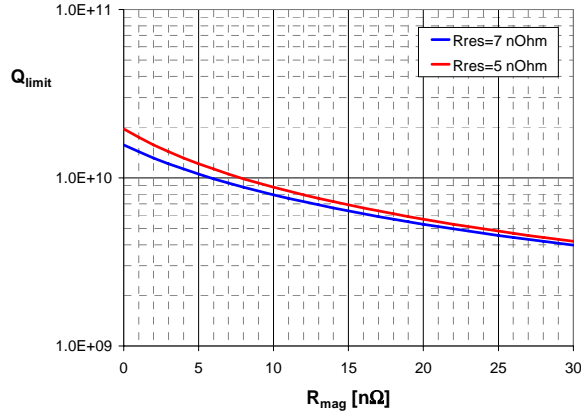


Figure 2: Cavity Q as a function of the contribution to surface resistance by trapped magnetic flux (R_{mag}).

Shield Design

The shield is composed by 1 mm thickness “CRYOPERM 10” sheets and it is located across the cavity, internal to the He tank. The shield is supported at the cavity tubes by means of small G10 blocks that separate the high permeability metal from the niobium surfaces at the tube to avoid any possible contact to the end irises which may occur at cold conditions due to the differential thermal shrinkage of materials.

The shield is composed of three parts (shown in Figure 3): a central tubular section enclosing all cells and two half closure parts at each end to limit the magnetic flux entering from the large diameter of the central section. The assembly allows the longitudinal adjustment to the final cavity length (for frequency tuning and field flatness) and can be laterally inserted from one side, where the smaller diameter He tank support dish is located.

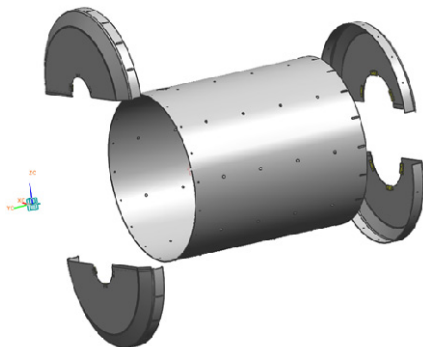


Figure 3: The parts of the cavity magnetic shield.

The end closure parts of the shield are shaped in order to keep them at a distance from the region where the weld to the He tank need to be performed, in order to limit the possibilities of heating them during the weld operations and deteriorate the high permeability of the material. Figure 4 shows the magnetic shield around the cavity prior to the sliding of the He tank before welding.



Figure 4: The shield around the cavity.

The slotted ends at the connections from the end shields to the tube allow the longitudinal adjustment to the final cavity length and provide a good contact between the different shield parts in order to avoid field leaking. Moreover, small (3 mm diameter) holes are foreseen on the shield tube to allow He gas flow during cooldown.

Shield Performances

To evaluate the shielding performances of the internal shield, we performed magnetic field measurements and compared the results with numerical studies [5].

Magnetic field map measurements were performed at different orientations of the shield with respect to the earth magnetic field, at the positions of the cavity irises and equators. These values were used to estimate the field along the cavity surface (red dots in Figure 5), the mean cavity surface field and the corresponding contribution to the surface resistance (line 2 of Table 1).

We then simulated the 1 mm thick Cryoperm shield in the $\sim 40 \mu\text{T}$ of the earth magnetic field. The measurements can be reproduced with a good approximation using a permeability $\mu_r = 15,000$, a value lower than the nominal $\mu_r = 70,000$ of the heat treated material, accounting for small gaps, and deterioration occurring during assembly. The computed field along the cavity surface is shown in Figure 5 (continuous blue line) while the mean cavity surface field and the corresponding contribution to the surface resistance, according to equation 2, are summarized in Table 1 (line 1).

Table 1: mean surface magnetic field and contribution to surface resistance

	$\langle H \rangle \text{ (}\mu\text{T)}$	$R_s \text{ (n}\Omega\text{)}$
Simulated case ($\mu_r = 15,000$)	3.35	8.44
Measured case	3.70	9.33

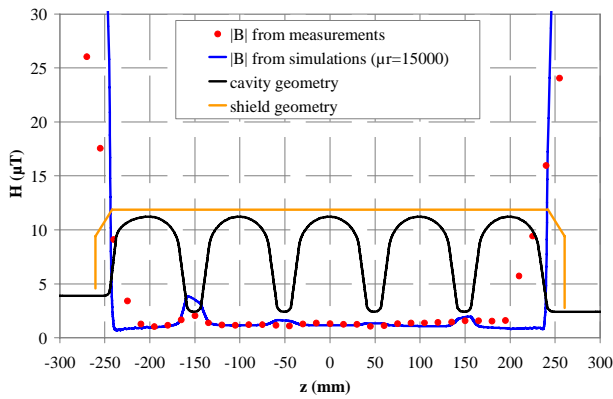


Figure 5: Magnetic field on the cavity surface from simulations and field map measurements. The black solid line indicates the cavity geometry and the orange line shows the magnetic shield geometry.

Figure 5 shows a good agreement between the calculated data and the measured values along the cavity surface: in both cases the contribution to the surface resistance by trapped magnetic field is estimated to be below 10 nΩ, which guarantees the goal Q value with a comfortable operational margin.

FINAL INTEGRATION AND TUNING

The two TRASCO cavities have been integrated in their Helium tanks with different orientations of the coupler port to the horizontal plane: in CRYHOLAB the coupler is oriented horizontally, while for the prototypical cryomodule of the EUROTRANS program the coupler is oriented vertically.

Final Integration

After the magnetic shield installation the final integration of the cavity to the Helium tank has been performed. The procedure requires performing two electron beam (EB) weld operations (to connect the Ti tank parts to the Ti end dishes of the cavity) and one TIG weld (under protected Ar conditions) to perform the last orbital weld of the two portions of the tank that allow the length adjustment to the cavity.

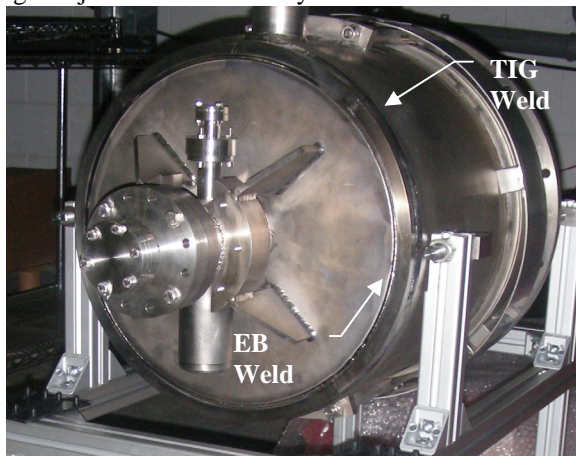


Figure 6: Cavity-Tank welded connection.

Before the cavity integration in the Helium tank the cavities were tuned to field flatness (a level of 3.8% and 4.5% of out-of flatness was reached during the tuning).

During the tank integration welding procedure the field flatness of the cavity was measured several times, in order to verify the possible occurrence of plastic cavity deformations during the process.

Field Flatness Measurements after Integration

Cavity Z502 was first integrated in the tank. A field flatness decrease (up to 14.8% of field unbalance) was observed soon after the mechanical fitting of the tank. This suggests a loss of planarity between the cavity end dishes, which forced a slight bending of the multicell structure to allow the fitting. Subsequent weld operations did not further deteriorate the situation. The planarity loss probably originated during the pretuning procedure that was needed to match the cavity nominal frequency. When cavity Z501 was integrated in the He tank, only a minor modification was induced on the field flatness, causing the field unbalance to rise from 3.8 to 6.4%.

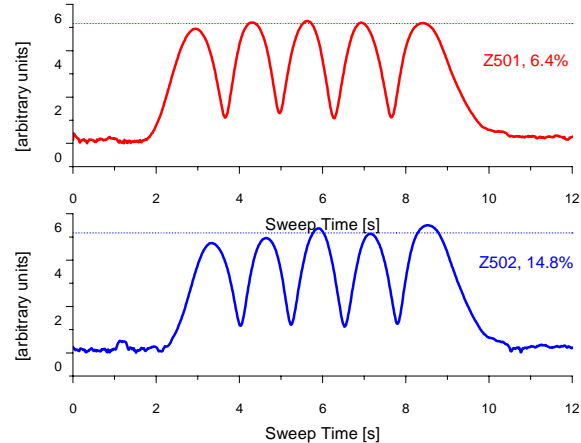


Figure 7: Field flatness after final integration of the two cavities, Z501 and Z502.

CONCLUSIONS

The TRASCO cavities have been equipped with a magnetic shield, a Helium tank and a cold motor system to allow horizontal testing in pulsed and CW conditions. So far all components are up to specifications and system tests will be performed in the near future.

REFERENCES

- [1] D. Barni et al., in Proceedings of EPAC 2000, Vienna, Austria, p. 2019.
- [2] P. Pierini et al., CARE-Note-2006-003-HIPPI.
- [3] P. Pierini et al., in Proceedings of EPAC 2008, Genova, Italy, p. 898
- [4] A. Bosotti et al., in Proceedings of EPAC 2004, Lucerne, Switzerland, p. 1024.
- [5] R. Paparella et al., in these Proceedings, WE5PFP032.
- [6] H. Padamsee, J. Knobloch, T. Hays, “RF Superconductivity for Accelerators”, John Wiley and Sons, New York, 1998.